Rapid Lewis Acid Screening and Reaction Optimization using 3D Printed Catalyst Impregnated Stirrer Devices in the Synthesis of Heterocycles

Rumintha Thavarajah,[a] Matthew R. Penny,[a] Ryo Torii[b] and Stephen T. Hilton[a]*

[a] Department of Pharmaceutical and Biological Chemistry, UCL School of Pharmacy, 29-39 Brunswick Square, London, WC1N 1AX United Kingdom.
[b] Department of Mechanical Engineering, UCL, Torrington Place, London WC1E 7JE

ABSTRACT: We describe the development of Lewis Acid catalyst-impregnated 3D printed stirrer devices and demonstrate their ability to facilitate the rapid screening of reaction conditions to synthesize heterocycles. The SLA 3D printed stirrer devices were designed to fit round-bottomed flasks and Radleys carousel-tubes using our recently reported solvent resistant resin and using CFD modelling studies and experimental data, we demonstrated that the device design leads to rapid mixing and rapid throughput over the device surface. Using a range of Lewis Acid 3D printed stirrers, the reaction between a diamine and an aldehyde was optimized for catalyst and solvent and we demonstrated that use of the 3D printed catalyst embedded devices led to higher yields and reduced reaction times. A library of benzimidazole and benzothiazole compounds were synthesized and use of devices led to efficient formation of the product as well as low levels of catalyst in the resultant crude mixture. The use of these devices makes the process of setting up multiple reactions simpler by avoiding weighing out of catalysts and the devices, once used, can be simply removed from the reaction, making the process of compound library synthesis more facile.

Additive Manufacturing (AM),[1,2] also known as three-dimensional (3D) printing, is a versatile technique by which complex 3D objects can be created from a digital design with precise geometry.[3] Over the past decade, 3D printing has been established as a revolutionary tool for the chemical and pharmaceutical industries and other scientific disciplines.[1-9] The technique of 3D printing has grown in the field of chemistry following research by ourselves and others, where it has been shown to be an essential tool for the design, development and production of low-cost laboratory equipment, continuous flow systems and teaching aids.[1,3,10,11]

Despite the clear advantages of stereolithography (SLA) 3D printing over fused deposition modelling (FDM) in terms of accuracy and reproducibility, the use of SLA 3D printing in chemistry remains limited. This in part stems from the paucity of solvent resistant commercial resins that are available for SLA printing.[11j] However, recent research by our group into catalyst embedded stirrer devices for chemical synthesis has led to the discovery of a resin formulation that is stable to a range of organic solvents and that can be 3D printed with embedded Pd catalysts and that was shown to efficiently catalyze Suzuki-Miyaura reactions with low catalyst loss.[12]

As a result of our research into 3D printing and 3D printed catalyst embedded stirrers, we were intrigued by the possibility of extending our research into the area of Lewis Acids (LA), where LA catalysts could be incorporated into SLA 3D printed stirrer devices. Solid supported Lewis Acids have previously been used in the synthesis of heterocycles and active pharmaceutical ingredients (APIs),[13] but whilst they have been used in this approach, they typically require weighing out before use, in much the same way as the use of traditional solution-based catalysts.[13] Our new paradigm approach therefore provides a much more simplified workflow,[12] where a range of Lewis Acid impregnated stirrers can be readily added to a reaction followed by the reagents. Once the reaction is complete, they can then be removed at the end of the reaction in much the same way as a stirrer bar, making the entire process much simpler to follow, (Figure 1).

Figure 1: Illustration of standard chemical workflow (Top) versus our approach via the use of 3D printed catalyst embedded stirrer devices (Bottom).

As a proof of concept, we were interested in applying our approach using 3D printed Lewis Acid impregnated stirrer beads to the synthesis of benzimidazoles and

benzothiazoles and related derivatives due to their potent biological and pharmaceutical properties.[14] Both of these key heterocycles and related derivatives display numerous therapeutic activities such as: anti-cancer,[15] anti-fungal,[16] anti-flammatory,[17,18] anti-microbial,[19] anti-viral,[20,21] anti-HIV,[22] anti-bacterial,[23] and anti-ulcer effects.[24] The aim of our approach, was to demonstrate that the stirrer devices containing a range of catalysts, could then be used in a Radleys carousel to optimise the reaction scope for both catalyst and solvent, simplifying the workflow in catalyst screening.[25] In this manner, we would therefore be able to carry out the reaction with six or twelve stirrer devices at any one time, without the need to weigh out catalyst (Figure 2).
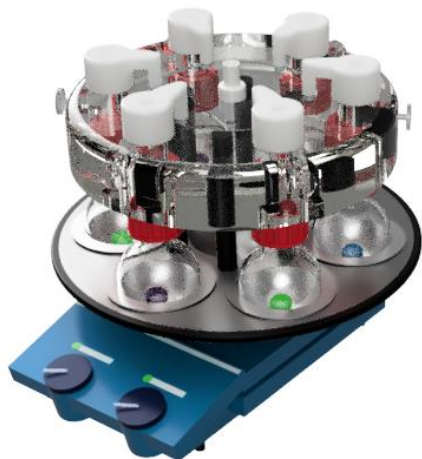

Figure 2: CAD drawing illustration of the use of a range of 6 different Lewis Acid Impregnated devices (coloured) in a Radleys Carousel reactor with the top made opaque for clarity.

To exemplify our approach, we explored the 3D printing of a range of Lewis Acid catalyst containing devices, covering Scandium, Ytterbium, Indium, Zinc, Copper (I) and Yttrium. Catalysts 2.5% (*w/w* versus resin) were dissolved in PEGDA monomer, photoinitiator added and the resultant devices 3D printed on a Formlabs Form1+ 3D printer to give the resultant catalyst embedded devices and rare earth stirrer beads inserted into the central cavity of the device as shown (Figure 3 and Supplementary Information). The weight and the amount of catalyst in each 3D printed stirrer device was calculated from 3D printing of the devices in triplicate, with an average weight range of 770 mg – 940 mg and a catalyst loading ranging from 19 mg – 23 mg depending on the catalyst (supplementary Information). There is a slight variation in the standard error of the mean of less than 0.5% for all catalysts examined, suggesting good size uniformity of the 3D printed stirrer devices. It is also evident from the uniform green color of the CuOTf impregnated stirrer device that there was successful dispersion of the catalyst throughout the device in all cases where the catalysts were soluble in the 3D printing resin.
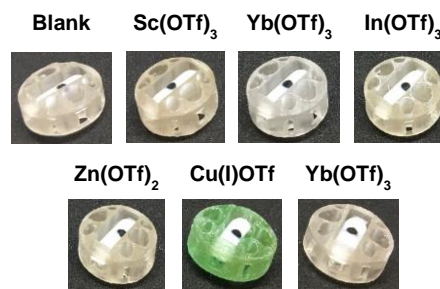

Figure 3: 3D Printed stirrer devices containing Lewis Acids.

In order to test the efficacy of our 3D printed stirrer devices, initial investigations focussed on exploring the effect of stirring, which was conducted through measuring the vortex height capabilities of each device. A Radleys carousel vial was placed in a 3D printed vial holder with a ruler set up on a stirrer hotplate to ensure that the vial was kept in the middle of the stirrer hot plate so that no variation in both the magnetic field and in the height of the vial occurred during repeat runs (Figure 4A). During this analysis, EtOH (5 mL and 10 mL) was placed in the carousel vial along with a blank 3D printed stirrer device and the resultant vial placed in the 3D printed holder containing a ruler. This was placed on a stirrer hot plate and the initial height measured from the bottom of the carousel tube to the top of the solvent level. While stirring at each RPM, the final height was measured from the bottom of the carousel tube to the top of the solvent level. The difference in final height and the initial height was measured as the vortex height (Figure 4B).
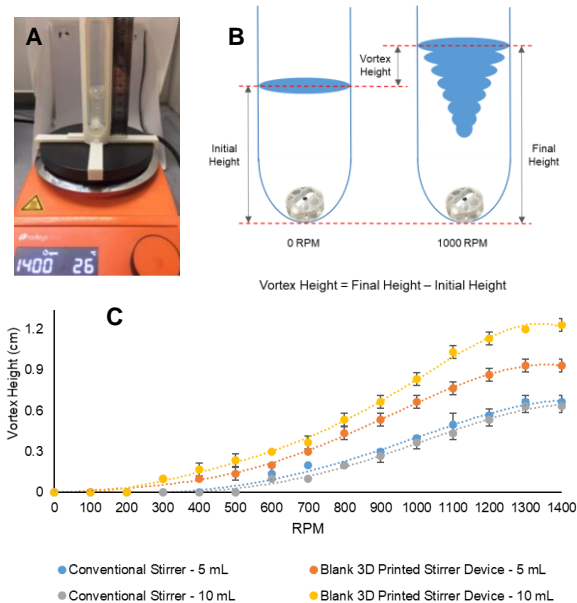

Figure 4: The investigation into the stirring effects. B: Illustration of how the vortex height was calculated. C: A direct comparison of the vortex capabilities of a conventional stirrer and a blank 3D printed carousel/ RBF stirrer device in 5 mL and 10 mL of EtOH using a carousel vial (20 mL).

The stirring ability of the 3D printed stirrer device greatly exceeded that of the conventional stirrer with

both 5 mL and 10 mL of solvent (Figure 4C). The vortex height of both stirrers remained similar from 0-200 RPM, however, from 300 RPM the difference in vortex height of the 3D printed stirrer devices steadily increased, whilst the conventional stirrer remained at zero until 500 RPM. Increasing the volume of EtOH to 10 mL led to a steeper increase in turbulence. The high vortex abilities measured for the 3D printed stirrer over that of its simple bar congener device can be visualised below, showing the increased turbulence exerted by the device (Figure 5).

Figure 5: The vortexing ability of a conventional stirrer at 1400 rpm (left) versus that of its 3D printed congener (right).

To corroborate the vortexing height capability findings, a modelling study comparing the mixing ability of a blank 3D printed stirrer device against a conventional magnetic stirrer was conducted using EtOH (5 mL) with a density of 0.7893 g/cm^3 and a viscosity of 1.074 mPa-s. At time equal to zero, the temperature of the air was set to 25 °C with no observed surface tension at the interface. The results from the simulation of simplified fluid dynamics clearly agreed with the experimental findings, in that the 3D printed device displays a higher degree of rapid mixing with greater turbulence, (Figure 6 and Supplementary Information).
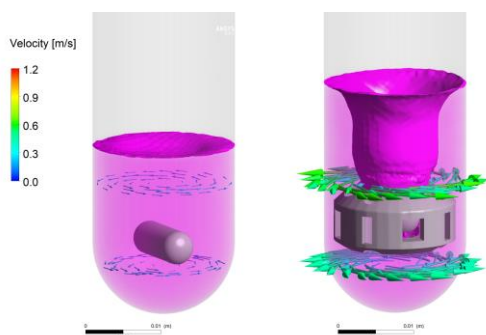

Figure 6: The computational analysis of the vortexing ability of a conventional stirrer at 1400 rpm (left) versus that of its 3D printed congener (right).

The average swirling flow velocity magnitude in the two planes at t = 5s is greater in the 3D printed stirrer device than the conventional stirrer. The velocity for the

3D printed stirrer device on the top and bottom plane is 0.0234 m/s and 0.407 m/s respectively, which is 2.5 times greater than the velocity experienced with the conventional stirrer. The flow is sucked in from the region below and ejected sideways through the lateral opening (Figure 7 and Supplementary Information). The colour contour represents the phases, where red is EtOH and blue represents the air. The volumetric flow rates coming through different openings are discrete; the green openings have the lowest flow rate of 0.212 mL/s but the red and side openings have the highest flow rate of 1.48 mL/s and 1.13 mL/s respectively. The total flow through the 3D printed stirrer device is 12.5 mL/s. Therefore, it shows that the 3D printed stirrer device does indeed exhibit an increased degree of mixing and greater turbulence in comparison to the commercially available conventional bar stirrer.
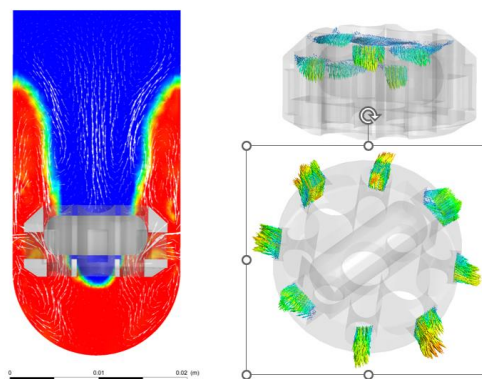

Figure 7: Modelling of the vortexing ability of the 3D printed stirrer and an illustration of the fluid flow through the device.

Following the results of the mixing tests in the carousel tubes, we wanted to explore the ability of the impregnated catalysts in the formation of substituted benzimidazoles following a report by Fan et al. on the use of Lewis Acids to facilitate the formation of benzimidazoles, we wanted to show how we could quickly and efficiently improve the reaction using our approach (Scheme 1).[26]
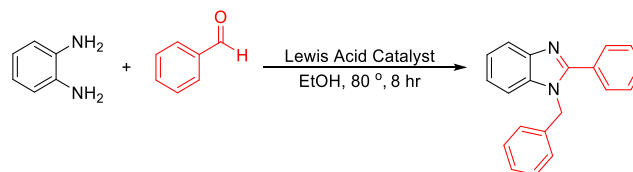
Scheme 1. Reaction of benzene-1,2-diamine and benzaldehyde in the presence of various Lewis Acid catalysts in EtOH.

The 3D Printed Lewis Acid catalyst impregnated devices screened in our study were: $Sc(OTf)_3$, $Yb(OTf)_3$, $In(OTf)_3$, $Zn(OTf)_2$, $Sc(OTf)_3$, CuOTf and $Y(OTf)_3$. The screened catalysts were heated at reflux in a Radleys

carousel tubes in EtOH for eight hours under inert conditions (Scheme 1). An initial background reaction with no catalyst and a conventional magnetic stirrer bar was run as a control and gave a low yield of the product (6%). Surprisingly, when the control reaction was repeated using a blank 3D printed stirrer, a yield of 14% was achieved. We attributed this increase in yield due to the rapid mixing abilities of the 3D printed stirrer devices in comparison to the conventional magnetic stirrer bar (Table 1).

Table 1. A = Conventional stirrer + powdered catalyst (0.1 mmol, 0.049 g) B = Blank 3D printed stirrer device + powdered catalyst (0.1 mmol, 0.049 g) C = Lewis acid catalyst impregnated 3D printed stirrer device. * = RBF, ** = no catalyst added.

	Form of Catalyst					
	A		B		C	
Normal Stirrer			6**			
Blank 3D Stirrer			14**			
Sc(OTf)$_3$	61	62*	64	65*	78	74*
Yb(OTf)$_3$	37		54		71	
In(OTf)$_3$	49		63		65	
Zn(OTf)$_2$	38		53		57	
CuOTf	25		33		38	
Y(OTf)	23		25		34	

(Isolated Yield (%))

From the results, we can clearly see that Sc(OTf)$_3$ proved to be the best catalyst for the synthesis of 2,3-disubstituted benzimidazoles and that in all cases, the use of the 3D printed catalyst impregnated device gave the highest yields in all the reactions despite the fact that the amount of catalyst in the catalyst impregnated stirrer device is a lot less in comparison to the powdered catalyst used (~20 mg versus ~48 mg). The stirrers possess a surface area of 1266 mm^2 and a volume of 646 mm^3, giving a surface area/ volume ratio of 2.0 mm^{-1}. However, the catalyst itself is distributed evenly throughout the device, meaning that only the catalyst near the surface is available for reaction.[12] As such, we estimate that only 10% of the actual catalyst is available for reaction for the carousel stirrer devices. The Sc(OTf)$_3$ impregnated stirrer device has approximately 20 mg of Sc(OTf)$_3$ where as in the reaction 49 mg has been used as a powdered catalyst. The reaction with Sc(OTf)$_3$ was also repeated in a round bottom flask (RBF) to further investigate whether similar yields can be achieved in a different vessel and we were pleased to note that this was the case.

It is worth mentioning that the work-up procedure was obviated in the reactions performed using the catalytic devices, as the 3D printed catalyst embedded device could be simply removed from the reaction mixture upon completion, whereas work-up was mandatory in

the reactions catalyzed by powdered Lewis Acid catalysts.

A solvent screening test was subsequently carried out using the scandium triflate impregnated 3D printed stirrer devices. From the results, acetonitrile was found to be the optimum solvent, giving the highest yield and the shortest reaction times (Table 2). Pleasingly, the use of polar and non-polar solvents did not affect the architecture of stirrer devices, with the structural integrity maintained even at temperatures of 100 °C.

Table 2. Screening of polar and non-polar solvents to optimise the reaction conditions.

Solvent	Temperature of Reaction (° C)	Time of Reflux (hr)	Isolated Yield (%)
MeCN	80	2	87
MeCN	80	4	84
MeCN	80	6	79
MeCN (dry)	80	6	71
MeCN + H$_2$O (4:1)	80	6	52
EtOH	80	2	51
EtOAc	80	6	55
MeOH (dry)	80	6	82
t-butanol	80	6	68
IPA	80	6	65
H$_2$O	100	6	42
THF (dry)	80	6	27
Toluene	100	6	63

Following the selection of the optimised conditions, comparative reactions were carried out to try to understand the relative advantages of the stirrer devices as opposed to normal stirrers. Reactions without any catalyst using both conventional and blank 3D printed stirrer devices, gave 0% yield at the end of the reaction. We calculated that there is 20.3 mg of Sc(OTf)$_3$ in each device, so a comparative reaction was also carried out using 20.3 mg of powdered catalyst, which gave a 63% yield. Use of the catalyst impregnated stirrer device gave the highest yield of 87% (Scheme 2, Table 3).
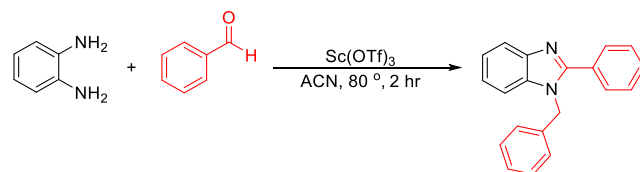

Scheme 2. Optimised reaction condition for the synthesis of 1-benzyl-2-phenyl-1*H*-benzo[*d*]imidazole using benzene-1,2-diamine, benzaldehyde and Sc(OTf)$_3$ as the catalyst in MeCN.

Table 3. Isolated yields obtained from different forms of catalysts.

Form of catalyst	% Isolated Yield
Normal stirrer	0
3D Blank Stirrer	0
Normal Stirrer + 0.049 mg cat.	68
Normal Stirrer + 0.020 mg cat.	63
3D Blank Stirrer + 0.049 mg cat.	79
3D Blank Stirrer + 0.020 mg cat	76
3D Sc(OTf)$_3$ Impregnated Stirrer	87

A reusability test was carried out using a Sc(OTf)$_3$ impregnated 3D printed stirrer device. The device was washed in the reaction solvent, dried and used in the same reaction using the same substrate and reaction molarities. The yields of the reaction are consistent for the first two repeats: 83% and 86% respectively, with yields dropping from the third repeat (Table 4 and Supplementary Information).

Table 4. Reusability test with a Sc(OTf)$_3$ impregnated stirrer.
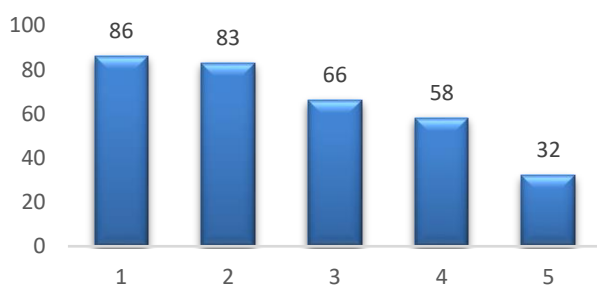
From the results (Supplementary Information), it was clear that the devices discolour rapidly after the second reaction presumably upon exposure to the diamine, with increasing morphological changes to the device after each repeat.

To understand whether the scandium was being lost to the reaction through leaching and catalysing the reaction in that manner, or whether the reaction was taking place at the surface of the device, an analysis of scandium leaching from the reaction was caried out, with detection from inductively coupled plasma optical emission spectroscopy (ICP-OES). Pleasingly, only 1% of the total amount of scandium catalyst was lost in the two-hour reaction when the catalyst impregnated 3D printed stirrer device was utilised (Table 5). This reduced leaching effect of the 3D printed stirrer devices and the fact that these devices can be reused, indicates that it may not be leaching effect and may also partly be due to surface phenomena. Therefore, it is safe to assume that it is not the leached material that is carrying out the reaction.
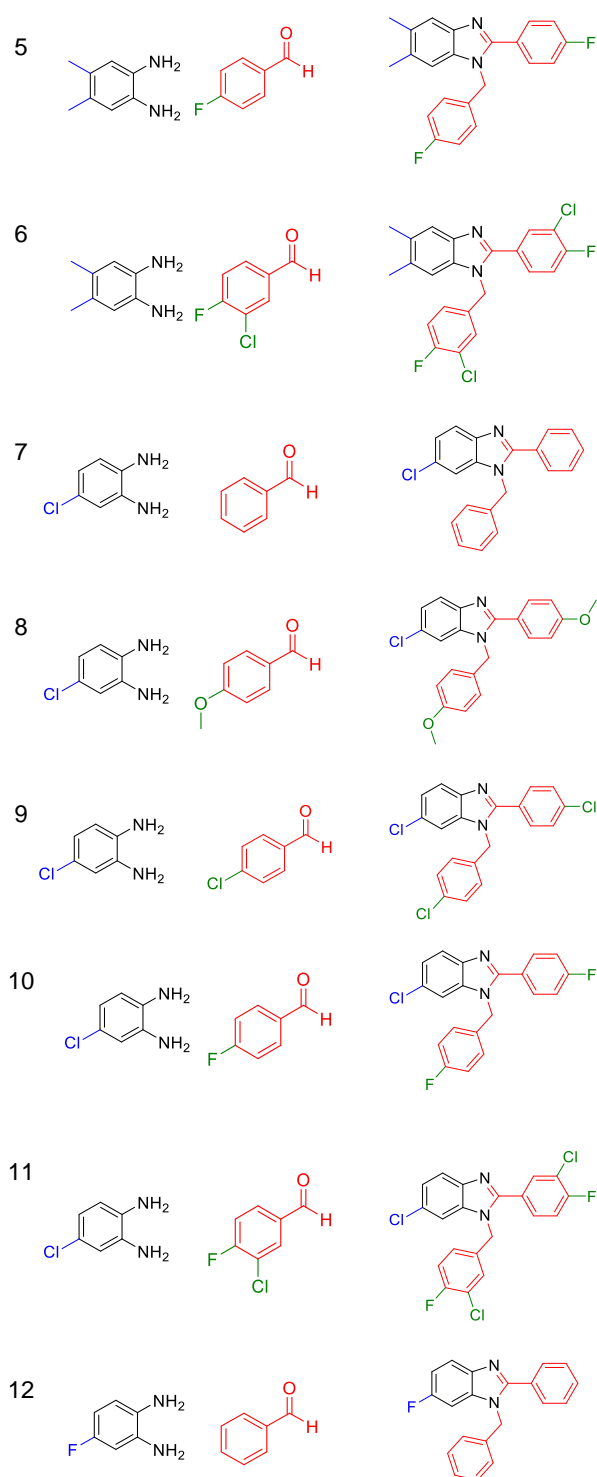
Table 5. ICP-MS study of scandium leaching in the reaction; A. no catalyst + blank 3D printed stirrer device, B. powdered catalyst + conventional magnetic stirrer, C. powdered catalyst + blank 3D printed stirrer device, D. Sc(OTf)$_3$ impregnated 3D printed stirrer device.

Entry	Mass of Sc metal used in the reaction (mg)	Mass of Sc metal detected through ICP-MS (mg)	Sc(OTf)$_3$ leached (%)
A	0.00	0.00	0
B	4.48	3.98	89
C	4.48	3.67	82
D	1.85	0.02	1

In order to demonstrate the utility of our approach, using the optimised reaction conditions, a library of benzimidazole compounds were synthesised using the scandium triflate impregnated 3D printed stirrer device in excellent yields (Table 6). A range of diamine and aldehyde derivatives were chosen to investigate the level of tolerance of the stirrer devices to different functional groups.

Table 6. Library of benzimidazole compounds using derivatives of diamine and aldehydes.

Entry	Diamine	Aldehyde	Product	Yield (%)
1				99
2				95
3				93
4				99

5

#	Yield
5	92
6	89
7	85
8	88
9	86
10	83
11	71
12	91

al. have recently reported on the use of Yttrium chloride to catalyze the reaction between *o*-aminothiophenol and benzaldehyde in the synthesis of benzthiazoles.[27] We were therefore interested in using YCl_3 as the catalyst in our resin formulation. However, due to the insoluble nature of YCl_3 in our resin formulation, we elected to use $YCl_3 \cdot 6H_2O$. A loading of 1% of the catalyst in the stirrer device was chosen to maintain consistency with powdered catalysts, enabling direct comparisons between the two variations of catalysts (Scheme 3).

$$YCl_3 \cdot 6H_2O \ (1\% \ (w/w))$$
EtOH, 85 °C, 2 hr
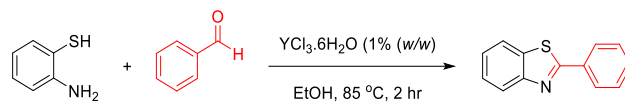
Scheme 3. The synthesis of 2-phenylbenzo[d]thiazole, $YCl_3 \cdot 6H_2O$ catalyzed *o*-aminothiophenol and benzaldehyde in EtOH.

We were interested in monitoring the progress of the above reaction using a 1% $YCl_3 \cdot 6H_2O$ impregnated stirrer device (including % conversion over the course of the reaction) to explore the potential of our 3D printed stirrers. As such, we carried out a series of reaction runs using conventional stirring, powdered catalyst and catalyst impregnated devices, with all reactions carried out in triplicate and the results of the reaction and the reaction profiles are shown below (Figure 8).
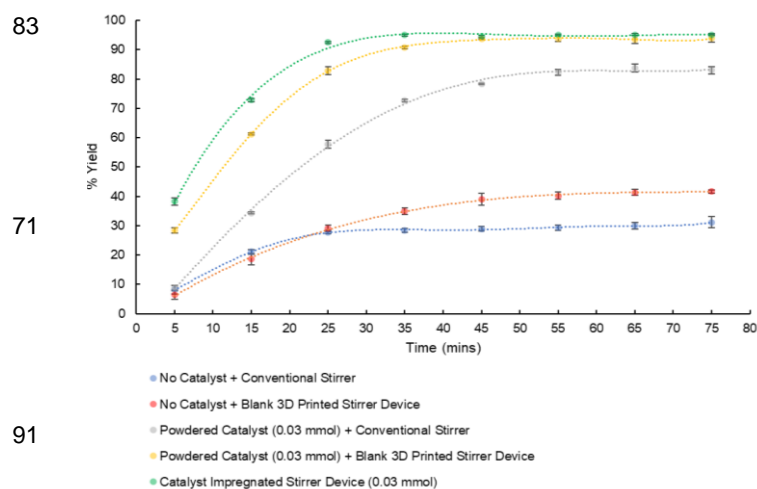
Figure 8: Monitoring the progress of reaction in the formation of 2-phenylbenzo[*d*]thiazole via LCMS analysis.

Pleasingly in all cases, the resultant benzimidazoles were obtained in good to excellent yields, demonstrating the tolerability of the devices towards an array of functional groups.

Having demonstrated the utility and application of the Lewis Acid catalyst embedded devices in optimizing reaction conditions, we next wanted to explore their utility in a previously reported LA catalysed reaction. Fan *et*

Both control reactions, without the use of any catalyst, showed conversion of product with 42% and 30% yield with the blank 3D printer stirrer device (red line) and conventional stirrer (blue line) respectively in 65 minutes. The significant difference between these two reactions highlights the effective mixing achieved with the 3D printer stirrer device. The reaction using the catalyst impregnated stirrer device (green line) went to

6

completion at 35 minutes in a yield of 95%. In comparison to all other reactions using different forms of catalysts, the catalyst impregnated stirrer device exhibited the fastest reaction rate and highest yield in the shortest time. Furthermore. a similar trend in the rate of reaction was observed when using the powdered catalyst in combination with the blank 3D printed stirrer device (yellow line), but with a slight increase in reaction time to 45 minutes. This close relationship is again associated with the high turbulence with the 3D printed stirrer devices. The reaction using powdered catalysts and conventional stirrer (grey line) displayed a significantly lower rate of reaction when compared with the catalyst impregnated stirrer device, and the longest reaction time (excluding controls) with a comparatively lower yield of 84% in 65 minutes. The reaction carried out with the impregnated device was also cleaner when analysed by LCMS when compared to its solution-based congener (Supplementary Information).

A reusability study of the $YCl_3.6H_2O$ impregnated stirrer devices was carried out, where the catalytic device was washed in the reaction solvent (EtOH), dried and used in the same reaction. The reusability for the first two repeats gave the product in good yields with 95% and 92% respectively and similar reaction profiles, but a profound difference in both the reaction rate and final yield was encountered during the third repeat. At the end of the 75-minute reaction, a yield of only 18% was recorded, implying that the catalytic device/ catalyst on the surface may have undergone degradation on exposure to reactants (Figure 9).
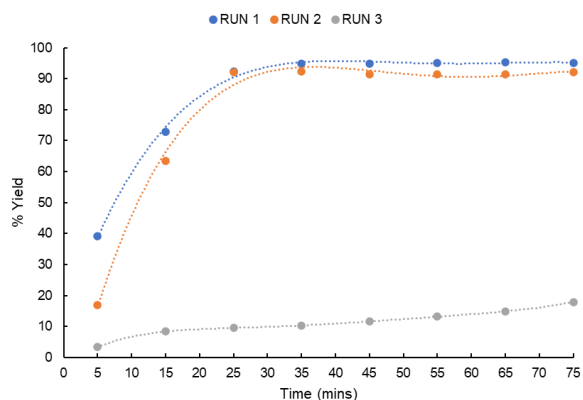
Figure 9: Reusability and reaction profile of the $YCl_3.6H_2O$ 3D printed devices.

To confirm that the change in reaction rate was due to the degradation/ poisoning of the catalyst and was not due to simple leaching, we investigated catalyst loss using ICP-MS (Table 7).
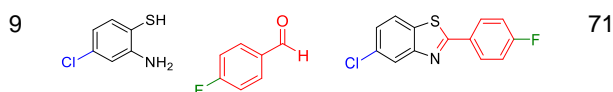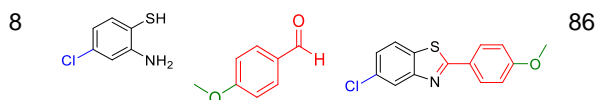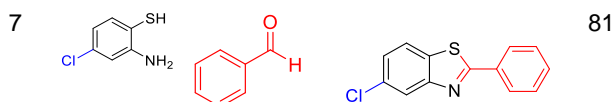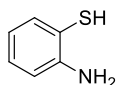
Table 7. ICP-MS study of yttrium leaching in the reaction; A. no catalyst + blank 3D printed stirrer device, B. powdered catalyst + conventional magnetic stirrer, C. powdered catalyst + blank 3D printed stirrer device, D. $YCl_3.6H_2O$ impregnated 3D printed stirrer device.

	Mass of Y metal used in the reaction (mg)	Mass of Y metal detected through ICP-MS (mg)	$YCl_3.6H_2O$ leached (%)
A	0.00	0.00	0
B	2.67 (in the stirrer device)	0.00560	0.21

From the results obtained, it can be seen that as with the Scandium impregnated devices, there is very little loss of Yttrium into the reaction medium. As such, it appears that the loss of activity in the third run is probably due to slow poisoning of the embedded catalyst on the surface of the device by the reactants. Having demonstrated the utility of the Yttrium impregnated stirrers, a library of benzothiazole compounds were synthesised in excellent yields (Table 8). A range of thiazole and aldehyde derivatives were chosen to investigate the level of tolerance of the stirrer devices to different functional groups.

Table 7. Library of benzothiazole compounds using derivatives of thiazoles and aldehydes.

	Thiazole	Aldehyde	Product	Yield (%)
1				93
2				97
3				89
4				87
5				74
6				85

7

AUTHOR INFORMATION

Corresponding Author

Dr Stephen Hilton – email: s.hilton@ucl.ac.uk

Author Contributions

The manuscript was written through contributions of all authors. / All authors have given approval to the final version of the manuscript.

All reactions gave good yields of the substituted benzothiazoles and avoided extensive purification due to the clean nature of the reaction via catalysis from the YCl$_3$ embedded 3D printed devices clearly highlighting the utility of the LA impregnated devices.

In summary, we have demonstrated the significance of 3D printing in chemical synthesis to aid batch reactions through the development of novel 3D printed stirrer devices that contain Lewis Acids and demonstrated their clear advantages over normal batch catalysis. The preliminary investigations into the use of these 3D printed stirrer devices to optimise both reaction efficiency and reaction simplicity have shown that the efficient stirring of the devices allows for a greater interaction of the reactants in comparison to the traditional synthetic route involving powdered catalyst and conventional stirrer. The reactions of various benzene-1,2-diamines and *o*-aminothiophenols with various benzaldehydes in the presence of a range of Lewis Acid catalysts and solvents have been carried out and optimised reaction condition have been developed. The use of such devices omits the need for the weighing out of powdered catalysts and simplifies the work up procedure, thus saving time. The ability to reuse the stirrer devices has also been successfully demonstrated and further investigations as to the exact nature of the catalyst and investigation of the ranges of catalysts that can be impregnated into the stirrer devices will be reported in due course.

ASSOCIATED CONTENT

Supporting Information. Details of the production of the stirrer devices, their requisite printing, surface analysis, use and full experimental details are provided in the Supporting Information and this material is available free of charge via the Internet at http://pubs.acs.org."

REFERENCES

[1] Capel, A. J., Rimington, R. P., Lewis, M. P. & Christie, S. D. R. 3D printing for chemical, pharmaceutical and biological applications. *Nat. Rev. Chem.* **2**, 422–436 (2018).

[2] Rossi, S., Puglisi, A. & Benaglia, M. Additive Manufacturing Technologies: 3D Printing in Organic Synthesis. *ChemCatChem* **10**, 1512–1525 (2018).

[3] Kitson, P. J. *et al.* 3D printing of versatile reactionware for chemical synthesis. *Nat. Protoc.* **11**, 920–936 (2016).

[4] Ligon, S. C., Liska, R., Stampfl, J., Gurr, M. & Mülhaupt, R. Polymers for 3D Printing and Customized Additive Manufacturing. *Chemical Reviews* **117**, 10212–10290 (2017).

[5] Melchels, F. P. W., Feijen, J. & Grijpma, D. W. A review on stereolithography and its applications in biomedical engineering. *Biomaterials* **31**, 6121–6130 (2010).

[6] Jamróz, W., Szafraniec, J., Kurek, M. & Jachowicz, R. 3D Printing in Pharmaceutical and Medical Applications – Recent Achievements and Challenges. *Pharmaceutical Research* **35**, (2018).

[7] Marcoux, J. & Bonin, K. Three Dimensional Printing: An Introduction for Information Professionals. *ICDS 2012, Sixth Int. Conf.* 54–58 (2012).

[8] Penny, M. R. *et al.* Three-Dimensional Printing of a Scalable Molecular Model and Orbital Kit for Organic Chemistry Teaching and Learning. *J. Chem. Educ.* **94**, 1265–1271 (2017).

[9] Lee Ventola, C. Medical applications for 3D printing: Current and projected uses. *P T* **39**, 704–711 (2014).

[10] a) Rayna, T. & Striukova, L. From rapid prototyping

to home fabrication: How 3D printing is changing business model innovation. *Technol. Forecast. Soc. Change* **102**, 214–224 (2016); b) Penny, M., Cao, Z., Patel, B., Sil dos Santos, B., Asquith, C., Szulc, B. R., Rao, Z. X., Muwaffak, Z., Malkinson, J. P., Hilton, S. T. Three-Dimensional Printing of a Scalable Molecular Model and Orbital Kit for Organic Chemistry Teaching and Learning *J. Chem. Ed.*, **94**, 1265-1271 (2017).

[11] a) Baden, T. *et al.* Open Labware: 3-D Printing Your Own Lab Equipment. *PLoS Biol.* **13**, (2015); b) Gross, B. C.; Erkal, J. L.; Lockwood, S. Y.; Chen, C.; Spence, D. M. Evaluation of 3D printing and its potential impact on biotechnology and the chemical sciences. *Anal. Chem.*, **86**, 3240-3253 (2014); c) Kitson, P. J., Marshall, R. J., Long, D. , Forgan, R. S., Cronin, L. 3D printed high-throughput hydrothermal reactionware for discovery, optimization, and scale-up. *Angew. Chem. Int. Ed.*, **53**, 12723–12728 (2014); d) Ambrosi, A.; Pumera, M. 3D-printing technologies for electrochemical applications. *Chem. Soc. Rev.*, **45**, 2740–2755 (2016); e) Rossi, S.; Porta, R.; Brenna, D.; Puglisi, A.; Benaglia, M. Stereoselective Catalytic Synthesis of Active Pharmaceutical Ingredients in Homemade 3D-Printed Mesoreactors. *Angew. Chem. Int. Ed.* **56**, 4290–4294 (2017); f) Tyson, A. L.; Hilton, S. T.; Andreae, L.C. Rapid, simple and inexpensive production of custom 3D printed equipment for large-volume fluorescence microscopy. *Int. J. Pharm.* **494**, 651–656 (2015); Talapatra, S. K.; Penny, M. R.; Hilton, S. T.; Kozielski, F. Design, 3D printing and validation of a novel low-cost high-capacity sitting-drop bridge for protein crystallization. *J. Appl. Cryst.* **52**, 171-174 (2019); g) Rao, Z. X.; Patel, B.; Monaco, A.; Cao, Z. J.; Barniol-Xicota, M.; Pichon, E.; Ladlow, M.; Hilton, S. T. 3D Printed Polypropylene Continuous-Flow Column Reactors: Exploration of Reactor Utility in SNAr Addition Reactions and the Synthesis of Bicyclic and Tetracyclic Heterocycles. *Eur. J. Org. Chem.* 6499-6504 (2017); h) Van Melis, C. G. W.; Penny, M. R.; Garcia, A. D.; Petti, A.; Dobbs, A. P.; Hilton, S. T.; Lam, K. Supporting-Electrolyte-Free Electrochemical Methoxymethylation of Alcohols Using a 3D-Printed Electrosynthesis Continuous Flow Cell System. *ChemElectroChem*, **6**, 4144-4148 (2019); i) Penny, M. R.; Rao, Z. X.; Peniche, B. F.; Hilton, S. T. Modular 3D Printed Compressed Air Driven Continuous-Flow Systems for Chemical Synthesis. *Eur. J. Org. Chem,* **23***,* 3783-3787 (2019); j) Capel, A. J.; Rimington, R. P.; Lewis, M. P.; Christie, S. D. R. 3D printing for chemical, pharmaceutical and biological applications. *Nat. Rev. Chem.* **2**, 422-436 (2018).

[12] a) Penny, M. R.; Hilton, S.T. Design and Development of 3D Printed Catalytically-Active Stirrers for Chemical Synthesis *React. Chem. Eng.* **2020**, *5*, 853-858; b) Penny, M. R.; Rao Z. X.; Thavarajah, R.; Ishaq, A.;Hilton, S.T. 3D printed tetrakis(triphenylphosphine)palladium (0) impregnated stirrer devices for Suzuki–Miyaura cross-coupling reactions, *React. Chem. Eng.*, *https://doi.org/10.1039/D2RE00218C* (2022)*;* c) http://www.silverson.com/us/products/ultramix-mixers, accessed 25th September 2022.

[13] a) Gupta, P., Paul, S. Solid acids: green alternatives for acid catalysis, *Catalysis Today* **235**, 153-170 (2014); b) Bayat, M., Gheidari, D. green Lewis Acid catalysts in organic reactions. *ChemistrySelect* **7**, e202200774 (2022); c) Sloan, L. A., Procter, D. J. Lanthanide reagents in solid phase synthesis *Chem. Soc. Rev.* **35**, 1221-1229 (2006).

[14] Sivakumar, R. *et al.* Benzimidazole: An attractive pharmacophore in medicinal chemistry. *International Journal of Pharmaceutical Research* **3**, 19–31 (2011).

[15] Kamila, S., Koh, B. & Biehl, E. R. Microwave-assisted 'green' synthesis of 2-alkyl/arylbenzothiazoles in one pot: A facile approach to anti-tumor drugs. *J. Heterocycl. Chem.* **43**, 1609–1612 (2006).

[16] Singh, N. *et al.* Benzimidazole: A short review of their antimicrobial activities. *Int. Curr. Pharm. J.* **1**, 110–118 (2012).

[17] Salahuddin, Shaharyar, M. & Mazumder, A. Benzimidazoles: A biologically active compounds. *Arabian Journal of Chemistry* **10**, S157–S173 (2017).

[18] Ghonim, A. E. *et al.* Structure-activity relationships of thiazole and benzothiazole derivatives as selective cannabinoid CB2 agonists with in vivo anti-inflammatory properties. *Eur. J. Med. Chem.* **180**, 154–170 (2019).

[19] Singh, M., Singh, S. K., Gangwar, M., Nath, G. & Singh, S. K. Design, synthesis and mode of action of novel 2-(4-aminophenyl)benzothiazole derivatives bearing semicarbazone and thiosemicarbazone moiety as potent antimicrobial agents. *Med. Chem. Res.* **25**, 263–282 (2016).

[20] Srestha, N., Banerjee, J. & Srivastava, S. A review on chemistry and biological significance of benzimidaole nucleus. *IOSR J. Pharm.* **04**, 28–41 (2014).

[21] Vicini, P. *et al.* Synthesis and biological evaluation of benzo[d]isothiazole, benzothiazole and thiazole Schiff bases. *Bioorganic Med. Chem.* **11**, 4785–4789 (2003).

[22] Nagarajan, S. R. *et al.* Discovery of novel benzothiazolesulfonamides as potent inhibitors of HIV-1 protease. *Bioorganic Med. Chem.* **11**, 4769–4777 (2003).

[23]   Rajasekhar, S., Maiti, B., M. Balamurali, M. & Chanda, K. Synthesis and Medicinal Applications of Benzimidazoles: An Overview. *Curr. Org. Synth.* **14**, 40–60 (2016).

[24]   R.G., I. & D.D., M. Heterocyclic Chemistry of Benzimidazoles and Potential Activities of Derivatives. *Int. J. Drug Res. Technol.* **1**, 26–32 (2011).

[25]   https://www.radleys.com/product/carousel-12-plus-standard-system/?utm_source=GShopping&utm_campaign=GoogleAds&utm_source=Gpmax&utm_campaign=GoogleAds&creative=&keyword=&matchtype=&network=x&device=c&gclid=CjwKCAjwm8WZBhBUEiwA178UnIk-9Svw3Tk3-SN2xHW2CVvSHnj9wjx1DtnUFok0YJqCEJiMb4AZuRoCb80QAvD_BwE, acceessed 26/09/2022.

[26]   Fan, L., Kong, L. & Chen, W. Highly chemoselective synthesis of benzimidazoles in Sc(OTf)3-catalyzed system. *Heterocycles* **91**, 2306–2314 (2015).

[27]   Fan, L. Y., Shang, Y. H., Li, X. X. & Hua, W. J. Yttrium-catalyzed heterocyclic formation via aerobic oxygenation: A green approach to benzothiazoles. *Chinese Chem. Lett.* **26**, 77–80 (2015).